Electron-spin dynamics induced by photon spins

Heiko Bauke,[1,][*] Sven Ahrens,[1] Christoph H. Keitel,[1] and Rainer Grobe[1,2]

[1]Max-Planck-Institut für Kernphysik, Saupfercheckweg 1, 69117 Heidelberg, Germany
[2]Intense Laser Physics Theory Unit and Department of Physics,
Illinois State University, Normal, IL 61790-4560 USA
(Dated: October 17, 2014)

Strong rotating magnetic fields may cause a precession of the electron's spin around the rotation axis of the magnetic field. The superposition of two counterpropagating laser beams with circular polarization and opposite helicity features such a rotating magnetic field component but also carries spin. The laser's spin density, that can be expressed in terms of the laser's electromagnetic fields and potentials, couples to the electron's spin via a relativistic correction to the Pauli equation. We show that the quantum mechanical interaction of the electron's spin with the laser's rotating magnetic field and with the laser's spin density counteract each other in such a way that a net spin rotation remains with a precession frequency that is much smaller than the frequency one would expect from the rotating magnetic field alone. In particular, the frequency scales differently with the laser's electric field strength depending on if relativistic corrections are taken into account or not. Thus, the relativistic coupling of the electron's spin to the laser's spin density changes the dynamics not only quantitatively but also qualitatively as compared to the nonrelativistic theory. The electron's spin dynamics is a genuine quantum mechanical relativistic effect.

1.   Introduction

Driven by recent developments of novel light sources that envisage to provide field intensities in excess of 10^{20} W/cm^2 and field frequencies in the x-ray domain [1–6] relativistic light matter interaction has become an active field of experimental and theoretical research in recent years [7–9]. The spin degree of freedom of a bound or free electron may show nontrivial dynamics or may influence the electron's motion in laser fields at relativistic intensities. Spin effects for electrons in intense linearly polarized laser fields were studied in [10, 11]. Distinct spin dynamics has been found in the relativistic Rabi effect [12] as well as in the relativistic Kapitza-Dirac effect [13, 14]; in [15] collapse-and-revival dynamics for the spin evolution of laser-driven electrons was predicted at 10^{18} W/cm^2, and also the dynamics of plasmas can be modified by spin effects [16]. Furthermore, the spin orientation relative to the polarization of the driving laser field affects the ionization rate of highly charged ions [17], correlations between electron spin and photon polarization in bremsstrahlung have been measured [18] and pair-production rates differ for partices with spin one half and spin zero [19, 20].

Additionally, the electron also light carries angular momentum [21]. The (classical) densities of spin and orbital angular momentum of light can be expressed in terms of the laser's electromagnetic fields and potentials. Spin and orbital angular momentum of light are of particular interest in current research [22–25] and it appears natural to ask if the light's spin density or orbital momentum density can couple to massive particles causing observable effects. In a pioneering work by Beth [26]

circularly polarized light was transformed into linear polarization removing spin angular momentum from the light beam and giving a measurable torque. Furthermore, in [27] a coupling of the orbital angular momentum of light to microscopic (classical) objects causing rotational or spinning motion was demonstrated and in [28] a direct coupling between the angular momentum of light and magnetic moments was predicted by classical considerations.

In this contribution, we examine electrons and the quantum dynamics of their spin in a standing light wave formed by two counterpropagating laser beams with elliptical polarization. We will show that the electromagnetic wave's spin density couples to the electron's spin causing electron spin precession. This precession is identified as a genuine relativistic effect that can only be explained by treating the electron quantum mechanically and taking into account relativistic corrections to the Pauli equation. The predicted spin effect may be realized by employing hard x-ray laser pulses of ultra high power with a stable pulse shape over a few hundred or more cycles.

2.   Elliptically polarized laser beams

We consider an electron in two counterpropagating elliptically polarized laser beams with the same wavelength λ and the same amplitude $\hat{E}$ but having opposite helicity. The electric and magnetic field components of the individual beams are given by

$$\boldsymbol{E}_{1,2}(\boldsymbol{r}, t) = \hat{E}\left(\cos(kx \mp \omega t)\boldsymbol{e}_y + \cos(kx \mp \omega t \pm \eta)\boldsymbol{e}_z\right), \quad (1a)$$

$$\boldsymbol{B}_{1,2}(\boldsymbol{r}, t) = \frac{\hat{E}}{c}\left(\mp \cos(kx \mp \omega t \pm \eta)\boldsymbol{e}_y \pm \cos(kx \mp \omega t)\boldsymbol{e}_z\right),$$
$$(1b)$$

with the wave number $k = 2\pi/\lambda$, the angular frequency $\omega = kc$, the speed of light c, the position $\mathbf{r} = (x, y, z)^\top$, and the time t, and $\mathbf{e}_x$, $\mathbf{e}_y$, and $\mathbf{e}_z$ denoting unit-vectors along the coordinate axes. The parameter $\eta \in [0, \pi/2]$ determines the degree of ellipticity with $\eta = 0$ corresponding to linear polarization and $\eta = \pi/2$ to circular polarization. In the latter case, the total electric and the magnetic components $\mathbf{E}_1(\mathbf{r}, t) + \mathbf{E}_2(\mathbf{r}, t)$ and $\mathbf{B}_1(\mathbf{r}, t) + \mathbf{B}_2(\mathbf{r}, t)$ are parallel to each other and rotate around the propagation direction. The laser fields' intensity is independent of the ellipticity and equals $I = \varepsilon_0 c \hat{E}^2$.

The spin angular momentum of light can be associated with its circular or elliptical polarization. Introducing the Coulomb gauge magnetic vector potentials $\mathbf{A}_{1,2}$ of the fields (1)

$$\mathbf{A}_{1,2}(\mathbf{r}, t) = -\frac{\hat{E}}{\omega}\left(\mp \sin(kx \mp \omega t)\mathbf{e}_y \mp \sin(kx \mp \omega t \pm \eta)\mathbf{e}_z\right) \quad (2)$$

we find that each laser field carries a spin density of $\varepsilon_0 \mathbf{E}_{1,2} \times \mathbf{A}_{1,2} = \varepsilon_0 \hat{E}^2 \lambda \sin\eta\, \mathbf{e}_x/(2\pi c)$. Thus, the spin density of the two plane waves in (1) points along the propagation axis of the two waves and is proportional to the sine of the ellipticity parameter η. Note that the definition of the spin angular momentum of light has been discussed controversially in the literature [29] and the total photonic spin density is

$$\varepsilon_0 \mathbf{E}_1 \times \mathbf{A}_1 + \varepsilon_0 \mathbf{E}_2 \times \mathbf{A}_2 = \frac{\varepsilon_0 \hat{E}^2 \lambda \sin\eta}{\pi c}\mathbf{e}_x, \quad (3)$$

which is compatible with a now commonly accepted definition of the photonic spin density [30–33] but it does *not* equal

$$\varepsilon_0 \mathbf{E} \times \mathbf{A} = 2\cos^2 kx\, \frac{\varepsilon_0 \hat{E}^2 \lambda \sin\eta}{\pi c}\mathbf{e}_x, \quad (4)$$

where $\mathbf{E} = \mathbf{E}_1 + \mathbf{E}_2$ and $\mathbf{A} = \mathbf{A}_1 + \mathbf{A}_2$ denote the total electric field and the total magnetic vector potential. Nevertheless, the quantity $\varepsilon_0 \mathbf{E} \times \mathbf{A}$ is meaningful for characterizing the electromagnetic field's degree of polarization because it equals (3) on average over a wavelength.

3. Numerical simulations and results

Due to the nonrelativistic electron velocities we assume that the fields act on the electron but there is no backreaction of the electron to the laser fields. This allows us to treat the electromagnetic fields via the classical vector potential $\mathbf{A}(\mathbf{r}, t)$. The evolution of the electron of mass m and charge $q = -e$ in the laser field, however, will be described fully quantum mechanically via the Dirac equation

$$i\hbar\dot{\Psi}(\mathbf{r}, t) = \left(c\boldsymbol{\alpha} \cdot \left(-i\hbar\boldsymbol{\nabla} - q\mathbf{A}(\mathbf{r}, t)\right) + mc^2\beta\right)\Psi(\mathbf{r}, t) \quad (5)$$

with the Dirac matrices $\boldsymbol{\alpha} = (\alpha_x, \alpha_y, \alpha_z)^\top$ and β [34, 35]. The combined vector potential of the two counterpropagating elliptically polarized fields (1) is given by

$$\mathbf{A}(\mathbf{r}, t) = -\frac{2w(t)\hat{E}}{\omega}\cos kx\,(\sin\omega t\, \mathbf{e}_y + \sin(\omega t - \eta)\,\mathbf{e}_z), \quad (6)$$

where we have deliberately introduced the window function

$$w(t) = \begin{cases} \sin^2 \frac{\pi t}{2\Delta T} & \text{if } 0 \leq t \leq \Delta T, \\ 1 & \text{if } \Delta T \leq t \leq T - \Delta T, \\ \sin^2 \frac{\pi(T-t)}{2\Delta T} & \text{if } T - \Delta T \leq t \leq T, \end{cases} \quad (7)$$

which allows for a smooth turn-on and turn-off of the electromagnetic fields. The variables T and ΔT denote the total interaction time and the time of turn-on and turn-off.

Taking into account the quasi one-dimensional sinusoidal structure of the vector potential (6) allows us to cast the partial differential equation (5) into a set of coupled ordinary differential equations [14]. For this purpose, we make the ansatz

$$\Psi(\mathbf{r}, t) = \sum_{n,\gamma} c_n^\gamma(t)\psi_n^\gamma(\mathbf{r}) \quad (8)$$

with $\gamma \in \{+\uparrow, -\uparrow, +\downarrow, -\downarrow\}$ and the basis functions

$$\psi_n^\gamma(\mathbf{r}) = \sqrt{\frac{k}{2\pi}}\, u_n^\gamma e^{inkx}, \quad (9)$$

with u_n^γ defined as

$$u_n^{+\uparrow/+\downarrow} = \sqrt{\frac{\mathcal{E}_n + mc^2}{2\mathcal{E}_n}}\begin{pmatrix} \chi^{\uparrow/\downarrow} \\ \frac{nck\hbar\sigma_x}{\mathcal{E}_n + mc^2}\chi^{\uparrow/\downarrow} \end{pmatrix}, \quad (10a)$$

$$u_n^{-\uparrow/-\downarrow} = \sqrt{\frac{\mathcal{E}_n + mc^2}{2\mathcal{E}_n}}\begin{pmatrix} -\frac{nck\hbar\sigma_x}{\mathcal{E}_n + mc^2}\chi^{\uparrow/\downarrow} \\ \chi^{\uparrow/\downarrow} \end{pmatrix}, \quad (10b)$$

$\chi^\uparrow = (1, 0)^\top$ and $\chi^\downarrow = (0, 1)^\top$, the Pauli matrix σ_x, and the relativistic energy momentum relation $\mathcal{E}_n = \sqrt{(mc^2)^2 + (nck\hbar)^2}$. The basis functions (10) are common eigenfunctions of the free Dirac Hamiltonian, the canonical momentum operator, and the Foldy-Wouthuysen spin operator [36]. Thus, $\psi_n^{+\uparrow}(\mathbf{r})$ and $\psi_n^{+\downarrow}(\mathbf{r})$ have positive energy $\mathcal{E}_n$ each and positive and negative spin one half, respectively, with respect to the z axis. Introducing the quadruples $c_n(t) = (c_n^{+\uparrow}(t), c_n^{+\downarrow}(t), c_n^{-\uparrow}(t), c_n^{-\downarrow}(t))^\top$ yields from (5) and (8) the Dirac equation in momentum space

$$i\hbar\dot{c}_n(t) = \mathcal{E}_n\beta c_n(t) + \sum_{n'} V_{n,n'}(t)c_{n'}(t), \quad (11)$$

with the interaction Hamiltonian $V_{n,n'}(t)$ and its components

$$V_{n,n'}^{\gamma,\gamma'}(t) = \frac{w(t)q\hat{E}}{k}\left(\delta_{n,n'-1} + \delta_{n,n'+1}\right) \times$$
$$\left(u_n^{\gamma\dagger}\alpha_y u_{n'}^{\gamma'}\sin\omega t + u_n^{\gamma\dagger}\alpha_z u_{n'}^{\gamma'}\sin(\omega t - \eta)\right). \quad (12)$$

The electron is initially at rest with spin aligned to the z axis, which corresponds to the initial condition $c_0^{+\uparrow}(0) = 1$ and $c_n^\gamma(0) = 0$ else. We solve the Dirac equation (11) numerically [14] starting from this initial condition and calculate the spin expectation value

$$s_z(T) = \frac{\hbar}{2}\sum_n |c_n^{+\uparrow}(T)|^2 + |c_n^{-\uparrow}(T)|^2 - |c_n^{+\downarrow}(T)|^2 - |c_n^{-\downarrow}(T)|^2 \quad (13)$$

after the field's amplitude dropped to zero at time $t = T$.[37]
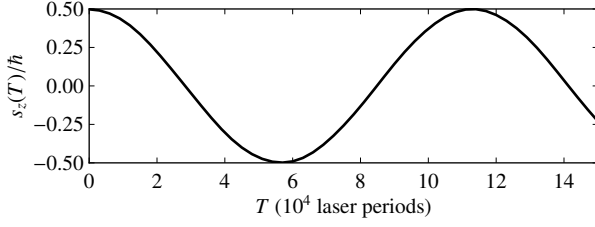
FIG. 1: Expectation value of the quantum mechanical electron spin in z direction $s_z(T)$ as a function of the total interaction time T. The wavelength and the amplitude of the applied circularly polarized fields is $\lambda = 0.992$ Å and $\hat{E} = 1.38 \times 10^{14}$ V/m, respectively, and the laser's switch-on-off interval ΔT corresponds to 20 laser cycles.
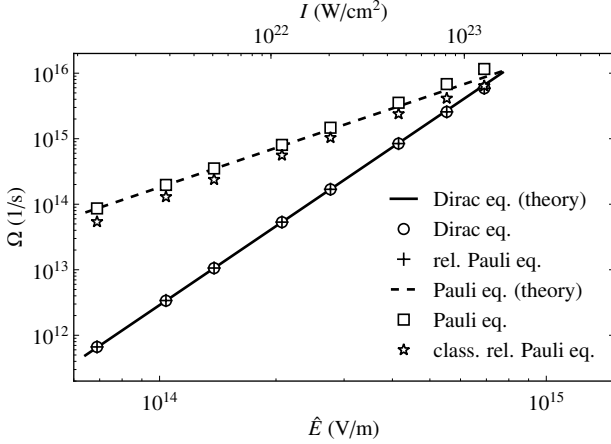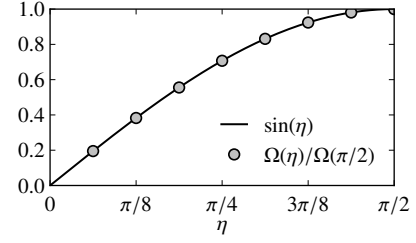

FIG. 2: Angular frequency Ω of the spin precession as a function of the laser's electric field strength $\hat{E}$ and its intensity I for lasers of the wavelength $\lambda = 0.992$ Å. Depending on the applied theory (the Dirac equation (5), the relativistic Pauli equation (16), the nonrelativistic Pauli equation, or the classical equation (22)) the spin of an electron in two counterpropagating circularly polarized light waves scales with the second or fourth power of $\hat{E}$. Theoretical predictions for the spin-precession frequency are given by (14) and (19), respectively.

Let us consider the special case of circular polarization first. As shown in Fig. 1 the expectation value $s_z(T)$ oscillates periodically with a period much larger than the laser's period, i. e., it does not just follow the field adiabatically. The spin's expectation value in the y direction oscillates in a similar fashion but with a $\pi/2$ phase shift. Thus, the electron's spin precesses around the x axis, i. e., the propagation direction of the laser field. Considering the interaction Hamiltonian $V_{n,n'}(t)$ as a perturbation to the free Dirac Hamiltonian, time-dependent perturbation theory [14] for the Dirac equation (11) yields the angular frequency Ω of the spin precession for the case of circular polarization

$$\Omega = \frac{(q\hat{E})^4 \lambda^5}{(2\pi)^5 \hbar^2 m^2 c^5} \,. \tag{14}$$

One can show that the application of perturbation theory is justified provided that both inequalities $|q|\hat{E} < k^2\hbar c$ and $|q|\hat{E} < 2kmc^2$ hold. A comparison of this prediction for the spin-precession angular frequency with results from the numer-

FIG. 3: Spin-precession angular frequency Ω (normalized to the precession frequency for circular light) as a function of the ellipticity parameter η. The electric field strength was set to $\hat{E} = 5.53 \times 10^{14}$ V/m; other parameters as in Fig. 1.

ical solution of the Dirac equation (11) shows a good agreement between theory and simulations, see black solid line and circles in Fig. 2. In particular, the numerical results confirm that the spin-precession angular frequency Ω growths with the *fourth* power of the electric field strength $\hat{E}$.

While Figs. 1 and 2 show results for circular polarization Fig. 3 demonstrates the effect of an ellipticity parameter $\eta \neq \pi/2$ by showing the spin-precession angular frequency Ω as a function of η. Our numerical results indicate that Ω is proportional to $\sin \eta$. Thus, the spin-precession angular frequency for electrons in counterpropagating elliptically polarized laser fields is proportional to the product of the laser field's intensity and the spin density of the electromagnetic wave.

4. Electron dynamics in the weakly relativistic limit

The Dirac equation (5) describes the fully relativistic quantum dynamics of the electron. It is, however, not very transparent when it comes to physical interpretation. It is a standard procedure to consider a nonrelativistic expansion of the Dirac equation via a Foldy-Wouthuysen transformation [36, 38]. The resulting expansion

$$
\begin{aligned}
i\hbar\dot{\Psi}(\boldsymbol{r},t) = \Bigg(& \frac{(-i\hbar\boldsymbol{\nabla} - q\boldsymbol{A}(\boldsymbol{r},t))^2}{2m} - \frac{q\hbar}{2m}\boldsymbol{\sigma}\cdot\boldsymbol{B}(\boldsymbol{r},t) + q\phi(\boldsymbol{r},t) \\
& - \frac{(-i\hbar\boldsymbol{\nabla} - q\boldsymbol{A}(\boldsymbol{r},t))^4}{8m^3c^2} - \frac{q^2\hbar^2}{8m^3c^4}(c^2\boldsymbol{B}(\boldsymbol{r},t)^2 - \boldsymbol{E}(\boldsymbol{r},t)^2) \\
& + \frac{q\hbar}{8m^3c^2}\left\{\boldsymbol{\sigma}\cdot\boldsymbol{B}(\boldsymbol{r},t), (-i\hbar\boldsymbol{\nabla} - q\boldsymbol{A}(\boldsymbol{r},t))^2\right\} \\
& -\frac{q\hbar}{4m^2c^2}\boldsymbol{\sigma}\cdot(\boldsymbol{E}(\boldsymbol{r},t)\times(-i\hbar\boldsymbol{\nabla} - q\boldsymbol{A}(\boldsymbol{r},t))) - \frac{q\hbar^2}{8m^2c^2}\boldsymbol{\nabla}\cdot\boldsymbol{E}(\boldsymbol{r},t)\Bigg)\Psi(\boldsymbol{r},t)\,.
\end{aligned}
\tag{15}
$$

with $\boldsymbol{A}$ given by (6), $\boldsymbol{B} = \boldsymbol{\nabla}\times\boldsymbol{A}$, $\boldsymbol{E} = -\dot{\boldsymbol{A}}$, and the Pauli matrices $\boldsymbol{\sigma} = (\sigma_x, \sigma_y, \sigma_z)^\top$ allows for a manifest interpretation of the individual corrections to the nonrelativistic Pauli equation. The relativistic corrections $\sim (-i\hbar\boldsymbol{\nabla} - q\boldsymbol{A})^4$ and $\sim \boldsymbol{\nabla}\cdot\boldsymbol{E}$ (the so-called Darwin term) account for relativistic mass effects and field inhomogeneities, respectively, and the contribution $\sim \boldsymbol{\sigma}\cdot(\boldsymbol{E}\times(i\hbar\boldsymbol{\nabla}))$ leads to the well-known spin-orbit effect, while

$\boldsymbol{\sigma} \cdot (\boldsymbol{E} \times \boldsymbol{A})$ couples the photonic spin density to the electronic spin.

Conjecturing that the electromagnetic field's spin density is the only source for relativistic effects in the electron's spin dynamics, we consider now the relativistic Pauli equation where only the relativistic correction due to the field's spin density is included, i. e.,

$$i\hbar\dot{\Psi}(\boldsymbol{r},t) = \left(\frac{1}{2m}(-i\hbar\boldsymbol{\nabla} - q\boldsymbol{A}(\boldsymbol{r},t))^2 - \frac{q\hbar}{2m}\boldsymbol{\sigma}\cdot\boldsymbol{B}(\boldsymbol{r},t) \right.$$
$$\left. + \frac{q^2\hbar}{4m^2c^2}\boldsymbol{\sigma}\cdot(\boldsymbol{E}(\boldsymbol{r},t)\times\boldsymbol{A}(\boldsymbol{r},t)) \right)\Psi(\boldsymbol{r},t)\,. \quad (16)$$

This equation can be cast into a set of ordinary differential equations by a plane wave ansatz [14] similar to (8) for the Dirac equation. The angular frequency of the spin precession that results from a numerical solution of (16) agrees with the frequency from the full Dirac equation (5); see Fig. 2. This justifies our conjecture to utilize (16) as an effective equation for the full Dirac equation (5) and highlights the role of the electromagnetic field's spin density. Furthermore, the scaling of the spin-precession angular frequency changes qualitatively if the relativistic correction term in (16) is neglected. In fact, the spin-precession angular frequency scales with the *second* power of the electric field strength in this case; see squares in Fig. 2.

5. Classical electron-spin dynamics

The spin precession in the oscillatory field of the two counter-propagating elliptical laser fields may one remind on the Rabi effect [39]. This problem can be well understood by a classical model [40]. In the following we will adopt this approach to study spin precession in elliptical laser fields. For simplicity we assume circular polarization ($\eta = \pi/2$). The quantum state is delocalized over several laser wavelengths; thus we mimic the quantum wave packet by an ensemble of classical particles with spin angular momentum. These particles are placed along the x axis. The dynamics of a classical electron spin $\boldsymbol{s}$ at fixed position $\boldsymbol{r}$ in the magnetic field $\boldsymbol{B}(\boldsymbol{r},t) = \boldsymbol{B}_1(\boldsymbol{r},t) + \boldsymbol{B}_2(\boldsymbol{r},t)$ is governed by

$$\dot{\boldsymbol{s}}(t) = \frac{q}{m}\boldsymbol{s}(t)\times\boldsymbol{B}(\boldsymbol{r},t)\,. \quad (17)$$

This equation of motion can be justified via the Pauli equation, i. e., Eq. (16) neglecting the correction term that is proportional to $\boldsymbol{E} \times \boldsymbol{A}$, by calculating the quantum mechanical equation of motion for the spin observable in the Heisenberg picture [41]. For parameters such that $\Omega_\text{L} = q\hat{E}/(mc) \ll \omega$, where Ω_L denotes the oscillation frequency of a spin in a constant magnetic field with amplitude $\hat{E}/c$, the spin $\boldsymbol{s}(t)$ rotates with a position-dependent angular frequency around the axis of rotation of the magnetic field. For the initial condition $\boldsymbol{s}(0) = (0,0,\hbar/2)^\mathsf{T}$ the solution of (17) is given by

$$\boldsymbol{s}(t) = \frac{\hbar}{2}\left(0, \sin(2\Omega_\text{P}t\sin^2 kx), \cos(2\Omega_\text{P}t\sin^2 kx) \right)^\mathsf{T} \quad (18)$$

with the angular frequency averaged over a wavelength

$$\Omega_\text{P} = \frac{(q\hat{E})^2\lambda}{2\pi m^2 c^3}\,. \quad (19)$$

The frequency (19) agrees with the spin-precession angular frequency for the nonrelativistic Pauli equation that can be calculated via time-dependent perturbation theory and that is also confirmed by our numerical simulations; see squares in Fig. 2. Similarly, the relativistic correction in (16) to the Pauli equation leads to the classical equation

$$\dot{\boldsymbol{s}}(t) = -\frac{q^2}{2m^2 c^2}\boldsymbol{s}(t)\times(\boldsymbol{E}(\boldsymbol{r},t)\times\boldsymbol{A}(\boldsymbol{r},t))\,. \quad (20)$$

For the initial condition $\boldsymbol{s}(0) = (0,0,\hbar/2)^\mathsf{T}$ the solution of (20) is given by

$$\boldsymbol{s}(t) = \frac{\hbar}{2}\left(0, \sin(-2\Omega_\text{P}t\cos^2 kx), \cos(-2\Omega_\text{P}t\cos^2 kx) \right)^\mathsf{T}\,. \quad (21)$$

Note that due to the fast rotation of the magnetic field the net effect of the spin term proportional to $\boldsymbol{B}$ in (16) is of the same order as the relativistic correction proportional to $\boldsymbol{E} \times \boldsymbol{A}$. As a consequence of (18) and (21) a classical spin under the effect of both spin terms rotates in a short time interval Δt around the angle $2\Omega_\text{P}(\sin^2 kx - \cos^2 kx)\Delta t$. Averaged over a laser wavelength this rotation angle vanishes and the effects of the two spin terms chancel each other in our classical model. Thus, the classical model explains how the effect of the laser fields' spin density $\sim \boldsymbol{E} \times \boldsymbol{A}$ leads to a breakdown of the quadratic scaling of the spin-precession angular frequency in $\hat{E}$ that results if only the magnetic field is taken into account. The model, however, is not able to reproduce the quartic scaling in $\hat{E}$ that results from the fully relativistic quantum mechanical Dirac equation (5). The quartic scaling results as a genuine quantum effect from the fast temporal oscillations combined with the spatial modulation of the electromagnetic fields. Unlike the Rabi effect it does not solely result from the temporal oscillations of the electromagnetic fields.

In order to confirm that the precession frequency (14) is of quantum mechanical origin we also solved the coupled classical equations of motion for the spin $\boldsymbol{s}$, the position $\boldsymbol{r}$, and the canonical momentum $\boldsymbol{p}$ that correspond to the quantum mechanical Hamiltonian (16), namely

$$\dot{\boldsymbol{r}}(t) = \frac{\partial H(\boldsymbol{r},\boldsymbol{p})}{\partial\boldsymbol{p}}\,, \quad (22\text{a})$$

$$\dot{\boldsymbol{p}}(t) = -\frac{\partial H(\boldsymbol{r},\boldsymbol{p})}{\partial\boldsymbol{r}}\,, \quad (22\text{b})$$

$$\dot{\boldsymbol{s}}(t) = \frac{q}{m}\boldsymbol{s}(t)\times\boldsymbol{B}(\boldsymbol{r},t) - \frac{q^2}{2m^2 c^2}\boldsymbol{s}(t)\times(\boldsymbol{E}(\boldsymbol{r},t)\times\boldsymbol{A}(\boldsymbol{r},t))\,, \quad (22\text{c})$$

with

$$H(\boldsymbol{r},\boldsymbol{p}) = \left(\frac{1}{2m}(\boldsymbol{p} - q\boldsymbol{A}(\boldsymbol{r},t))^2 - \frac{q}{m}\boldsymbol{s}(t)\cdot\boldsymbol{B}(\boldsymbol{r},t) \right.$$
$$\left. + \frac{q^2}{2m^2 c^2}\boldsymbol{s}(t)\cdot(\boldsymbol{E}(\boldsymbol{r},t)\times\boldsymbol{A}(\boldsymbol{r},t)) \right)\,, \quad (22\text{d})$$

for the initial conditions $\boldsymbol{r}(0) = (0,0,0)^\mathsf{T}$, $\boldsymbol{p}(0) = (0,0,0)^\mathsf{T}$, and $\boldsymbol{s}(0) = (0,0,\hbar/2)^\mathsf{T}$. As we see in Fig. 2 the spin-precession frequency (stars) is reduced compared to (19) (dashed line) but also scales quadratically with the electric field amplitude.[42] The action of the magnetic field on the electron's spin is *not* canceled by the action due to the laser fields' spin-density because the time that the point-like electron spends in different regions of the laser field is not distributed uniformly over a laser wavelength.

6.   Experimental realization

Let us shortly estimate for what kind of laser parameters the electron's spin precession in elliptical fields may be observed. An experimental realization may utilize intense photon beams at nearfuture x-ray laser facilities to form standing waves. Intensity, frequency, and pulse length have to be carefully adjusted to make the spin precession detectable. For a given wavelength λ and pulse length n (number of cycles) the required electric field strength is bounded as

$$\left(\frac{(2\pi)^6 c^6 \hbar^2 m^2}{2nq^4\lambda^6}\right)^{1/4} < \hat{E} < \frac{(2\pi)^2 c\hbar}{|q|\lambda^2}. \tag{23}$$

In an experimental test of the predicted effect one has to detect a change of the electron's spin orientation, which must be large enough to be measurable. The lower bound in (23) results from the fact that at lower intensities the electron must be confined in the focus of the counterpropagating laser pulses for more cycles to realize a full spin flip. Note that the lower bound in (23) can be made arbitrarily small by inceasing the number of cycles n and/or raising the wavelength λ. Thus, the predicted coupling between electronic and photonic spins and the resulting electron spin precession are not intrinsic strong-field effects. Note that an increase of the wavelength may has to be accompanied by an extension of the pulse length n, otherwise the lower limit in (23) may exceed the upper limit. To give a specific numerical example, for $n = 5000$ the two bounds in (23) coincide for a wavelength of $\lambda = 0.24$ nm yielding $\hat{E} = 1.32 \times 10^{14}$ V/m and an intensity of $I = 4.64 \times 10^{21}$ W/cm^2. If the upper bound in (23) is violated the spin precession becomes anharmonic.

7.   Conclusions

We investigated electron motion in two counterpropagating elliptically polarized laser waves of opposite helicity and found

spin precession around the fields' propagation direction. The spin precession can be properly described via the fully relativistic Dirac equation or the nonrelativistic Pauli equation plus a relativistic correction proportional to $\boldsymbol{E} \times \boldsymbol{A}$. Because this quantity is closely related to the spin angular momentum of elliptically polarized light the relativistic correction can be interpreted as a coupling of the laser field's spin density to the electron spin. The spin-precession frequency is proportional to the product of the laser field's spin density and its intensity. The electron-spin dynamics has the remarkable feature that it is a genuine relativistic quantum effect. The quartic scaling of the spin-precession frequency with the electric field strength can not be found within the nonrelativistic Pauli theory; and also classical models that treat electrons as point-like particles fail to reproduce the correct spin-precession frequency even if relativistic effects due to the laser field's spin density are taken into account. This distinguishes the predicted spin effect from relativistic spin effects in other setups, e. g., in the Kapitza-Dirac effect [13, 14], where relativistic signatures are induced via relativistic system parameters, e. g., initial electron momenta.

We demonstrated that the coupling of the photonic spin to the electron's spin is closely related to the well-known spin-orbit effect. Both are examples for the interaction of two different kinds of angular momentum, a generic mechanism that can be observed also in very different contexts. For example, in [43] the interaction of the angular momentum of phonons in a magnetic crystal with the angular momentum of the crystal was recently considered and in [44] it is investigated how the orbital angular momentum of light affects the internal degrees of motion in molecules. In our setup of counterpropagating plane waves, the spin angular momentum is the electromagnetic field's only angular momentum. More realistic focused beams may also carry orbital angular momentum, which may also couple to the electronic spin and in this way modify the spin dynamics. Because of its fundamental nature we expect that the demonstrated coupling of the photonic spin to the electron's spin is of interest also for researchers beyond the strong field community.

Acknowledgments

[1] M. Altarelli, R. Brinkmann, M. Chergui, W. Decking, B. Dobson, S. Düsterer, G. Grübel, W. Graeff, H. Graafsma, J. Hajdu, J. Marangos, J. Pflüger, H. Redlin, D. Riley, I. Robinson, J. Rossbach, A. Schwarz, K. Tiedtke, T. Tschentscher, I. Vartaniants, H. Wabnitz, H. Weise, R. Wichmann, K. Witte, A. Wolf, M. Wulff, and M. Yurkov, eds., *The European X-Ray Free-Electron Laser Technical design report* (DESY XFEL Project Group European XFEL Project Team Deutsches Elektronen-Synchrotron Member of the Helmholtz Association, Hamburg, 2007).

[2] V. Yanovsky, V. Chvykov, G. Kalinchenko, P. Rousseau, T. Planchon, T. Matsuoka, A. Maksimchuk, J. Nees, G. Cheriaux, G. Mourou, and et al., Opt. Express **16**, 2109 (2008).

[3] B. W. J. McNeil and N. R. Thompson, Nat. Photonics **4**, 814 (2010).

[4] P. Emma, R. Akre, J. Arthur, R. Bionta, C. Bostedt, J. Bozek, A. Brachmann, P. Bucksbaum, R. Coffee, F.-J. Decker, Y. Ding, D. Dowell, S. Edstrom, A. Fisher, J. Frisch, S. Gilevich, J. Hastings, G. Hays, P. Hering, Z. Huang, R. Iverson, H. Loos, M. Messerschmidt, A. Miahnahri, S. Moeller, H.-D. Nuhn, G. Pile, D. Ratner, J. Rzepiela, D. Schultz, T. Smith, P. Stefan, H. Tompkins, J. Turner, J. Welch, W. White, J. Wu, G. Yocky, and J. Galayda, Nat. Photonics **4**, 641 (2010).

[5] G. Mourou and T. Tajima, Science **331**, 41 (2011).

[6] G. A. Mourou, N. J. Fisch, V. M. Malkin, Z. Toroker, E. A. Khazanov, A. M. Sergeev, T. Tajima, and B. Le Garrec, Opt. Commun. **285**, 720 (2012).

[7] T. Brabec, ed., *Strong Field Laser Physics*, Springer Series in Optical Sciences, Vol. 134 (Springer, Heidelberg, 2008).

[8] F. Ehlotzky, K. Krajewska, and J. Z. Kamiński, Rep. Prog. Phys. **72**, 046401 (2009).

[9] A. Di Piazza, C. Müller, K. Z. Hatsagortsyan, and C. H. Keitel, Rev. Mod. Phys. **84**, 1177 (2012).

[10] M. W. Walser, D. J. Urbach, K. Z. Hatsagortsyan, S. X. Hu, and C. H. Keitel, Phys. Rev. A **65**, 043410 (2002).

[11] M. Boca, V. Dinu, and V. Florescu, Nucl. Instrum. Methods Phys. Res., Sect. B **279**, 12 (2012).

[12] R. T. Hammond, Appl. Phys. Lett. **100**, 121112 (2012).

[13] S. Ahrens, H. Bauke, C. H. Keitel, and C. Müller, Phys. Rev. Lett. **109**, 043601 (2012).

[14] S. Ahrens, H. Bauke, C. H. Keitel, and C. Müller, Phys. Rev. A **88**, 012115 (2013).

[15] O. D. Skoromnik, I. D. Feranchuk, and C. H. Keitel, Phys. Rev. A **87**, 052107 (2013).

[16] G. Brodin, M. Marklund, J. Zamanian, and M. Stefan, Plasma Phys. Controlled Fusion **53**, 074013 (2011).

[17] M. Klaiber, E. Yakaboylu, C. Müller, H. Bauke, G. G. Paulus, and K. Z. Hatsagortsyan, J. Phys. B: At., Mol. Opt. Phys. **47**, 065603 (2014).

[18] S. Tashenov, T. Bäck, R. Barday, B. Cederwall, J. Enders, A. Khaplanov, Y. Poltoratska, K.-U. Schässburger, and A. Surzhykov, Phys. Rev. Lett. **107**, 173201 (2011).

[19] T. Cheng, M. R. Ware, Q. Su, and R. Grobe, Phys. Rev. A **80**, 062105 (2009).

[20] S. Villalba-Chávez and C. Müller, Phys. Lett. B **718**, 992 (2013).

[21] J. D. Jackson, *Classical Electrodynamics* (John Wiley & Sons, New York, 1998).

[22] M. Padgett and L. Allen, Contemp. Phys. **41**, 275 (2000).

[23] J. P. Torres and L. Torner, eds., *Twisted Photons: Applications of Light with Orbital Angular Momentum* (Wiley-VCH, Weinheim, 2011).

[24] D. L. Andrews and M. Babiker, eds., *The Angular Momentum of Light* (Cambridge University Press, Cambridge, 2012).

[25] I. Fernandez-Corbaton, X. Zambrana-Puyalto, and G. Molina-Terriza, Phys. Rev. A **86**, 042103 (2012).

[26] R. Beth, Phys. Rev. **50**, 115 (1936).

[27] H. He, M. E. J. Friese, N. R. Heckenberg, and H. Rubinsztein-Dunlop, Phys. Rev. Lett. **75**, 826 (1995).

[28] A. Raeliarijaona, S. Singh, H. Fu, and L. Bellaiche, Phys. Rev. Lett. **110**, 137205 (2013).

[29] M. Mansuripur, Phys. Rev. A **84**, 033838 (2011).

[30] A. M. Stewart, J. Mod. Opt. **52**, 1145 (2005).

[31] S. M. Barnett, J. Opt. (Bristol, U. K.) **13**, 064010 (2011).

[32] R. P. Cameron and S. M. Barnett, New J. Phys. **14**, 123019 (2012).

[33] K. Y. Bliokh, A. Y. Bekshaev, and F. Nori, New J. Phys. **15**, 033026 (2013).

[34] F. Gross, *Relativistic Quantum Mechanics and Field Theory* (Wiley-VCH, Weinheim, 2004).

[35] B. Thaller, *Advanced Visual Quantum Mechanics* (Springer, Heidelberg, 2005).

[36] L. L. Foldy and S. A. Wouthuysen, Phys. Rev. **78**, 29 (1950).

[37] The coefficients $c_n^{-\uparrow}(T)$ and $c_n^{-\downarrow}(T)$ are zero within numerical errors.

[38] J. Fröhlich and U. Studer, Rev. Mod. Phys. **65**, 733 (1993).

[39] I. I. Rabi, Phys. Rev. **51**, 652 (1937).

[40] L. Allen and J. H. Eberly, *Optical Resonance and Two-Level Atoms* (Dover, New York, 1987).

[41] A. J. Silenko, Phys. Rev. A **77**, 012116 (2008).

[42] The spin-precession frequency scales quadratically with the electric field amplitude even if higher relativistic corrections are taken into account via a classical equation given in [41].

[43] L. Zhang and Q. Niu, Phys. Rev. Lett. **112**, 085503 (2014).

[44] P. K. Mondal, B. Deb, and S. Majumder, Phys. Rev. A **89**, 063418 (2014).